The Astrophysical Journal Letters, 1000:L1 (6pp), 2026 March 20 https://doi.org/10.3847/2041-8213/ae4801
© 2026. The Author(s). Published by the American Astronomical Society.
OPEN ACCESS

Mass Measurements of the Double Neutron Star System PSR J0641+0448

Z. L. Yang[1,2], J. L. Han[1,3,2], P. F. Wang[1,2], C. Wang[1,3,2], N. N. Cai[1,2], W. C. Jing[1,3], W. Q. Su[1,2], T. Wang[1,2], J. Xu[1,2], Yi Yan[1,2], and D. J. Zhou[1,2]
[1] National Astronomical Observatories, Chinese Academy of Sciences, Jia-20 Datun Road, ChaoYang District, Beijing 100012, People's Republic of China; hjl@nao.cas.cn
[2] State Key Laboratory of Radio Astronomy and Technology, Beijing 100101, People's Republic of China
[3] School of Astronomy and Space Science, University of Chinese Academy of Sciences, Beijing 100049, People's Republic of China
Received 2026 January 6; revised 2026 February 18; accepted 2026 February 19; published 2026 March 11

Abstract

Pulsar timing of double neutron star (DNS) systems is one of the best methodologies to study the neutron star mass distribution. Here we report the discovery of a DNS system PSR J0641+0448 in the Five-hundred-meter Aperture Spherical radio Telescope (FAST) Galactic Plane Pulsar Snapshot survey. This pulsar has a 25.7 ms spin period and moves in a 3.73 day eccentric orbit with an eccentricity of 0.145. Using FAST observations, we obtained its phase-connected timing solution with periastron advance and Shapiro delay detected. Using χ^2 analysis based on the DDGR model, we constrain the pulsar mass to $1.319^{+0.021}_{-0.035}\,M_\odot$, and the companion mass to $1.269^{+0.022}_{-0.016}\,M_\odot$ with a 68.3% confidence level. The low companion mass and mild orbital eccentricity are consistent with the correlation between neutron masses and orbital eccentricities.

Unified Astronomy Thesaurus concepts: Binary pulsars (153); Relativistic binary stars (1386); Neutron stars (1108)

1. Introduction

The birth mass distribution of neutron stars represents a fundamental problem in binary pulsar population synthesis (T. M. Tauris & E. P. J. van den Heuvel 2023) and carries vital information about the supernova (SN) explosion mechanism (O. Pejcha et al. 2012). In binary systems, neutron star masses can increase through mass transfer processes such as wind accretion, Roche-lobe overflow, and common envelope evolution (T. M. Tauris & E. P. J. van den Heuvel 2023). Most binary pulsars are observed with low-mass companions, including He white dwarfs and low-mass main-sequence stars (R. N. Manchester et al. 2005). These systems descend from low-mass X-ray binaries, in which mass transfer proceeds over extended timescales, often leading to substantial mass growth of the pulsar (T. M. Tauris & E. P. J. van den Heuvel 2023). By contrast, double neutron star (DNS) systems experience only short-lived mass transfer episodes, yielding minimal increase in neutron star mass (T. M. Tauris et al. 2017). As a result, the mass of the first-born neutron star remains close to its birth value, while the second-born neutron star retains its original birth mass entirely. Given that, the mass distribution of Galactic DNS systems has been extensively investigated to constrain the birth mass distribution of neutron stars (F. Özel et al. 2012; F. Özel & P. Freire 2016; Z.-Q. You et al. 2025).

The potential to determine the masses of the pulsar and its companion through pulsar timing was recognized immediately after the discovery of the first DNS system (R. A. Hulse & J. H. Taylor 1975). These systems exhibit eccentric orbits and contain massive companions, which significantly facilitate the detection of relativistic effects. Such relativistic effects are described using post-Keplerian (PK) parameters (T. Damour & N. Deruelle 1985, 1986). When two or more PK parameters are measured, the component masses of the system can be determined within the framework of general relativity (T. Damour & J. H. Taylor 1992). Three or more PK parameters enable rigorous tests of gravitational theories, as demonstrated with exceptional precision in the double pulsar system PSR J0737–3039A/B (M. Kramer et al. 2021). So far, approximately 60 neutron stars have accurately measured masses,[4] many of which are also members of DNS systems. Despite that, yet a larger catalog of neutron star mass measurements remains essential.

Here we report the discovery of a DNS system, J0641+0448, identified by the Five-hundred-meter Aperture Spherical radio Telescope (FAST; R. Nan 2006; R. Nan et al. 2011) through its Galactic Plane Pulsar Snapshot (GPPS) survey (J. L. Han et al. 2021). The GPPS survey aims to discover pulsars within $\pm 10^\circ$ of the Galactic latitude from the Galactic plane in the sky visible to FAST and has so far detected over 800 new pulsars (J. L. Han et al. 2021, 2025), including three DNS systems: PSRs J0528+3529, J1844–0128, and J1901+0658 (W. Q. Su et al. 2024; P. F. Wang et al. 2025). PSR J0641+0448 is a mildly recycled pulsar with a spin period $P = 25.7$ ms, moving in a 3.73 day eccentric orbit ($e = 0.145$). The mass function implies a minimum companion mass of $1.28\,M_\odot$, indicating a massive companion and supporting the classification as a DNS system. Using more than 600 days of FAST observations, we have obtained a phase-connected timing solution and constrained the component masses of the system.

The structure of this Letter is as follows: Section 2 describes the discovery and follow-up observations of PSR J0641+0448; Section 3 presents the timing results and mass measurements; and Section 4 provides a discussion and conclusion of our findings.

Original content from this work may be used under the terms of the Creative Commons Attribution 4.0 licence. Any further distribution of this work must maintain attribution to the author(s) and the title of the work, journal citation and DOI.

[4] https://www3.mpifr-bonn.mpg.de/staff/pfreire/NS_masses.html

Table 1
Log of FAST Observations of PSR J0641+0448

Obs. Date (yyyymmdd)	Cover and Beam	Project ID	PI	Obs, Length (minutes)
20240516	G207.62+0.00M05P1	ZD2023_2	J.L. Han	5
20240608	J064133+044835M01	ZD2023_2	J.L. Han	15
20240629	J064133+044835M01	ZD2023_2	J.L. Han	15
20240811	J0641+0448gM01	ZD2024_2	J.L. Han	5
20250101	J0641+0448gM01	ZD2024_2	J.L. Han	10
20250205	J0641+0448gM01	ZD2024_2	J.L. Han	5
20250308	J0641+0448gM01	ZD2024_2	J.L. Han	5
20250612	J0641+0448gM01	ZD2024_2	J.L. Han	5
20250812	J0641+0448gM01	PT2025_0179	C. Wang	5
20250815	J0641+0448gM01	ZD2025_2	J.L. Han	5
20250822	J0641+0448M01	PT2025_0150	P.F. Wang	11
20250915	J0641+0448M01	PT2025_0150	P.F. Wang	10
20250930	J0641+0448M01	PT2025_0150	P.F. Wang	15
20251014	J0641+0448M01	PT2025_0161	P.F. Wang	10
20251104	J0641+0448M01	PT2025_0161	P.F. Wang	10
20251119	J0641+0448M01	PT2025_0161	P.F. Wang	10
20251205	J0641+0448M01	PT2025_0161	P.F. Wang	4
20251211	J0641+0448gM01	ZD2025_2	J.L. Han	10
20251215	J0641+0448gM01	ZD2025_2	J.L. Han	10
20251217	J0641+0448gM01	PT2025_0179	C. Wang	5
20251219	J0641+0448gM01	ZD2025_2	J.L. Han	10
20260101	J0641+0448gM01	ZD2025_2	J.L. Han	10
20260105	J0641+0448gM01	ZD2025_2	J.L. Han	10
20260205	J0641+0448gM01	ZD2025_2	J.L. Han	10
20260216	J0641+0448gM01	ZD2025_2	J.L. Han	10

Note. Listed are the Gregorian observation date, cover name jointed with FAST beam name, FAST project number, project principal investigator (PI), and observation length in minutes for each observation session.

2. FAST Observations and Data Reduction

2.1. FAST Observations of PSR J0641+0448

PSR J0641+0448 (GPPS No. 0670, originally designated PSR J0641+0448g in J. L. Han et al. 2025) was first detected in an 88 minute SnapShotZCal observation of the FAST GPPS survey on 2024 May 16. The detection was confirmed by a 15 minute tracking observation on 2024 June 8. To date, a total of 22 observational sessions have been carried out with FAST to study this source, which are listed in Table 1. All observations used the *L*-band 19-beam receiver, covering a frequency range from 1.0 to 1.5 GHz with a sampling time of 49.152 μs. The initial observation was recorded with 1024 frequency channels and 2 polarization channels (*XX* and *YY*), while all subsequent observations utilized 2048 frequency channels and 4 polarization channels (*XX*, *YY*, Re[*XY*], and Im [*XY*]). As part of the standard calibration procedure, a 2.01326 s period, 1.1 K modulated signal is injected into the receiver at either the beginning or the end of each FAST observation session.

2.2. Pulsar Timing and Polarization Profiles

We derived the barycentric spin period of PSR J0641+0448 at different barycentric epochs from each observation using PRESTO (S. M. Ransom 2001). The variation in the barycentric spin period indicates that the pulsar is in a binary system. Following the procedure described in P. F. Wang et al. (2025), which is based on the method introduced by B. Bhattacharyya & R. Nityananda (2008), we estimated the initial orbital parameters using the first eight observations.

Using these orbital parameters, we folded the raw *psrfits* data into pulse profiles with DSPSR (W. van Straten & M. Bailes 2011), adopting a subintegration length of 30 s. The resulting profiles were then calibrated and cleaned using the PSRCHIVE software package (A. W. Hotan et al. 2004). Under the ideal feed assumption, we folded the calibration signals and applied the corresponding calibration to the pulsar profiles using the `pac` command. Radio frequency interference was excised manually with the `psrzap` tool.

Subsequently, we reduced the data volume by averaging the full frequency channels into four sub-bands and the subintegrations into 300 s bins using the `pam` command. Times of arrivals (TOAs) were extracted from these integrated profiles with the `pat` command by cross-correlating them with a frequency-averaged one-dimensional template generated by `paas`. The dispersion measure (DM) value was refined by comparing TOAs from different sub-bands. Then we summed all frequency channels together and then regenerated the TOAs. The final number of TOAs is 44. We conducted pulsar timing using the TEMPO2 software package (G. B. Hobbs et al. 2006). The phase-connected timing solution for PSR J0641+0448 was obtained following the methodology outlined by P. C. C. Freire & A. Ridolfi (2018). The resulting timing model was then used to reprocess the observational data, yielding improved TOA measurements. The final timing solution was obtained based on these refined TOAs.

To derive the polarization profile, we first analyzed the 15 minute tracking observation from 2024 June 29 using the

Table 2
Timing Solution and Derived Parameters for PSR J0641+0448

General Information	
Pulsar name	J0641+0448
Data span (MJD)	60446 to 61088
Number of TOAs	44
$\chi^2/N_{\rm free}$	0.8407
Timescale	TCB
Solar system ephemeris model	DE440
Binary model	DD
Reference epoch (MJD)	60600
Measured Parameters	
Right ascension, α (J2000)	$06^{\rm h}41^{\rm m}34\overset{\rm s}{.}42114 \pm 0\overset{\rm s}{.}00008$
Declination, δ (J2000)	$04^\circ48'09\overset{''}{.}870 \pm 0\overset{''}{.}004$
Spin frequency, ν (s^{-1})	$38.94359974181 \pm 0.00000000003$
Derivative of spin frequency, $\dot{\nu}$ (s^{-2})	$(-9.95 \pm 0.05) \times 10^{-17}$
Dispersion measure, DM (pc cm^{-3})	155.185 ± 0.002
Rotation measure, RM (rad m^{-2})	136.7 ± 1.6
Orbital period, $P_{\rm orb}$ (d)	$3.73073229 \pm 0.00000004$
Epoch of periastron, T_0 (MJD)	$60601.646366 \pm 0.000004$
Projected semimajor axis of orbit, x (lt-s)	15.552366 ± 0.000011
Longitude of periastron, ω (deg)	5.1038 ± 0.0004
Orbital eccentricity, e	0.1454502 ± 0.0000003
Periastron advance, $\dot{\omega}$ (deg yr^{-1})	0.0427 ± 0.0003
Sine of orbital inclination, $\sin i$	0.98 ± 0.02
Companion mass, $M_{\rm c}$ ($M_\odot$)	1.3 ± 0.8
Derived Parameters	
Spin period, P (s)	$0.025678160381 42 \pm 0.00000000000002$
Spin period derivative, $\dot{P}$ (s s^{-1})	$(6.56 \pm 0.04) \times 10^{-20}$
Characteristic age, $\tau_{\rm c}$ (Gyr)	6.2
Surface magnetic field strength, $B_{\rm s}$ (G)	1.3×10^9
Mass function, f ($M_\odot$)	0.2901910 ± 0.0000007
DM derived distance, $d_{\rm NE2001}$ & $d_{\rm Y\ MW\ 16}$ (kpc)	5.3 & 2.6
Pulsar mass, $M_{\rm p}$ ($M_\odot$)[a]	$1.319^{+0.021}_{-0.035}$
Companion mass, $M_{\rm c}$ ($M_\odot$)[a]	$1.269^{+0.022}_{-0.016}$
Total mass, $M_{\rm tot}$ ($M_\odot$)[a]	$2.588^{+0.029}_{-0.031}$
Orbital inclination, i (deg)[a]	$79.6^{+2.7}_{-4.1}$

Notes. All listed uncertainties represent the 68.3% confidence level.
[a] Obtained via χ^2 analysis based on the DDGR model.

`rmfit` command, obtaining a Faraday rotation measure of $RM_{\rm obs} = 140.5 \pm 1.6$ rad m^{-2}. We then applied Faraday rotation correction via the `pam` command. Using the vertical total electron content maps of the ionosphere, CODE[5] and the International Geomagnetic Reference Field (IGRF-13)[6] with an updated code IONFR[7] (C. Sotomayor-Beltran et al. 2013), we determined the ionospheric contribution to the rotation measure to be 3.8 ± 0.3 rad m^{-2}. The intrinsic rotation measure of the pulsar is therefore 136.7 ± 1.6 rad m^{-2}. Following the same procedure, we applied Faraday rotation correction to each tracking observation and subsequently combined them using the `psradd` command. The resulting integrated polarization profile, along with the position angle of linear polarization at the infinite frequency, is shown in Figure 1.

[5] http://ftp.aiub.unibe.ch/CODE/
[6] https://www.ngdc.noaa.gov/IAGA/vmod/igrf.html
[7] https://sourceforge.net/projects/ionfarrot/

3. Timing Results and Mass Measurement

3.1. Timing Result

The timing solution for PSR J0641+0448 is presented in Table 2, with the corresponding timing residuals displayed in Figure 2. The absence of significant systematic trends in the residuals as a function of epoch or orbital phase indicates that the timing model provides a good fit to the data. The timing analyses are based on the Barycentric Coordinate Time (TCB) scale. We used the solar system ephemeris DE440 (R. S. Park et al. 2021) to correct the motion of FAST to the solar system barycenter. The orbital motion of the pulsar was modeled using the DD binary model (T. Damour & N. Deruelle 1985, 1986), which is widely adopted for DNS systems.

The pulsar has a characteristic age of 6.2 Gyr and a surface magnetic field strength of 1.3×10^9 G, values that are typical of a mildly recycled pulsar. Its Galactic longitude is $207\overset{\circ}{.}53441$ and Galactic latitude is $0\overset{\circ}{.}00106$. Using the NE2001 Galactic electron density model (J. M. Cordes & T. J. W. Lazio 2002), the distance derived from the DM is 5.3 kpc, whereas the

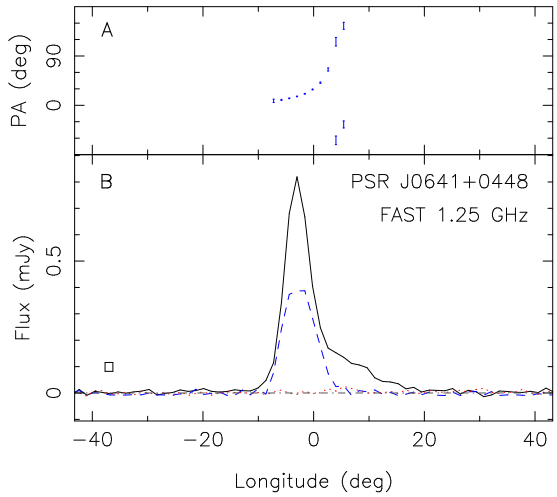


Figure 1. Polarization profiles of PSR J0653+0443. This was obtained by averaging all tracking observations of the pulsar, with an integration time of 215 minutes. Subpanel (A) is the position angles (PAs) of the linear polarization at the infinite frequency. The error bars indicate $\pm 1\sigma$ uncertainties. Subpanel (B) shows the total intensity I (black line), linear L (blue dashed line), and circular V (red dotted line, positive for the left-hand sense) polarization profiles, with a small square in the bottom left corner denoting $\pm 2\sigma_{\rm I,off}$ height and 1-bin width.

YMW16 model (J. M. Yao et al. 2017) yields 2.6 kpc. A future measurement of the orbital period derivative, which includes kinematic contributions from proper motion and Galactic acceleration, will help to constrain the system's distance and thereby improve the Galactic electron density model in this direction.

The timing solution yields precise Keplerian orbital parameters. From these, we derive the mass function, $f(M_{\rm p}, M_{\rm c}, \sin i)$, defined as

$$f(M_{\rm p}, M_{\rm c}, i) = \frac{(M_{\rm c}\sin i)^3}{(M_{\rm p}+M_{\rm c})^2} = \frac{4\pi^2}{G}\frac{x^3}{P_{\rm b}^2}, \quad (1)$$

where $M_{\rm p}$ and $M_{\rm c}$ are the masses of the pulsar and its companion, respectively, i is the orbital inclination angle, G is the gravitational constant, x is the projected semimajor axis of the pulsar's orbit, and $P_{\rm b}$ is the binary orbital period. Using the parameters from Table 2, we obtain a mass function of $0.290\,M_\odot$. This implies a minimum companion mass of $1.28\,M_\odot$ for an assumed pulsar mass of $M_{\rm p} = 1.4\,M_\odot$.

The periastron advance of this binary pulsar has been precisely measured, and in general relativity it is related to the total mass of the system $M_{\rm tot}$ as

$$\dot{\omega} = 3\left(\frac{P_{\rm orb}}{2\pi}\right)^{-5/3} G^{2/3} M_{\rm tot}^{2/3} c^{-2} (1-e^2)^{-1}. \quad (2)$$

Using the $\dot{\omega}$ value and uncertainty in Table 2, we found that the total mass of the system is $2.59 \pm 0.03\,M_\odot$.

For eccentric orbits, the Shapiro delay is expressed as (T. Damour & N. Deruelle 1986)

$$\Delta_{\rm S} = -\frac{2GM_{\rm c}}{c^3}\ln\{1 - e\cos u - \sin i[\sin\omega(\cos u - e) + \sqrt{1-e^2}\cos\omega\sin u]\}, \quad (3)$$

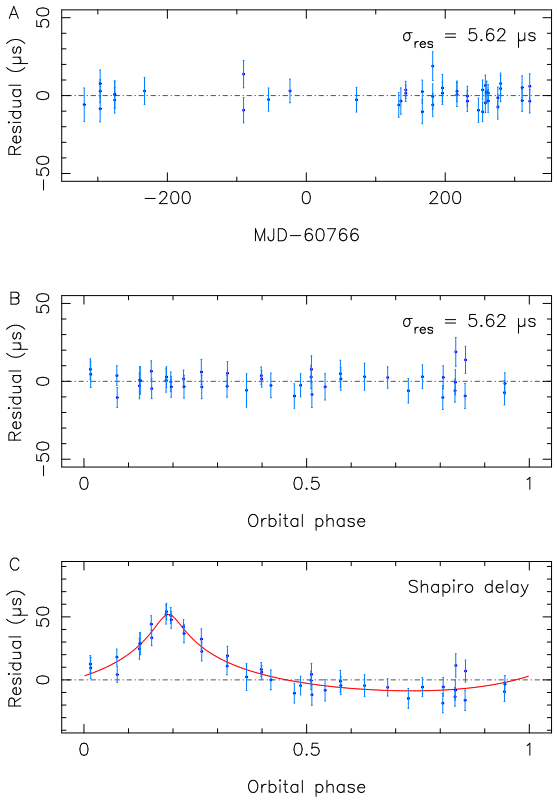


Figure 2. Timing residuals for PSR J0641+0448. The post-fit timing residuals are plotted versus epoch and orbital phase in subpanels (A) and (B), respectively. No systematic trends are apparent. The weighted rms of the residuals, $\sigma_{\rm res}$, is 5.62 μs. Subpanel (C) shows the Shapiro delay predicted by the best-fit values of the DDGR binary model ($M_{\rm c} = 1.269\,M_\odot$, $i = 79.^\circ6$).

where e is the orbital eccentricity and u is the eccentric anomaly. In PSR J0641+0448, the Shapiro delay was marginally detected (see Table 2).

3.2. Mass Measurement

Due to a mild orbital eccentricity of 0.145, we can assume that the spin axis of PSR J0641+0448 is aligned with the direction of orbital angular momentum (T. M. Tauris et al. 2017). Then, combined with the Keplerian orbital parameters in Table 2, under general relativity, all PK parameters in the DD binary model can be calculated using $M_{\rm p}$ and $M_{\rm c}$. We can combine all these relativistic effects together for the mass measurements, the realization of which is the DDGR binary model (J. H. Taylor 1987; J. H. Taylor & J. M. Weisberg 1989), where the fitting parameters are $M_{\rm c}$ and $M_{\rm tot}$ instead of PK parameters. Applying this binary model to PSR J0641+0448, TEMPO2 (G. B. Hobbs et al. 2006) reported $M_{\rm c} = 1.269 \pm 0.015\,M_\odot$ and $M_{\rm tot} = 2.588 \pm 0.030\,M_\odot$. These uncertainties are produced based on the approximation of linear propagation of uncertainties (G. B. Hobbs et al. 2006). However, the uncertainty of companion mass is significantly asymmetric, so this approximation is not sufficiently accurate.

Following E. M. Splaver et al. (2002), we employed a χ^2 analysis to better constrain the masses of PSR J0641+0448 and its companion. A uniform prior probability distribution was adopted in the $M_{\rm tot}$–$\cos i$ plane. Since the pulsar mass $M_{\rm p}$ must exceed 1 $M_\odot$, the corresponding gray region in Figure 3(A) is excluded. For each pair of trial values

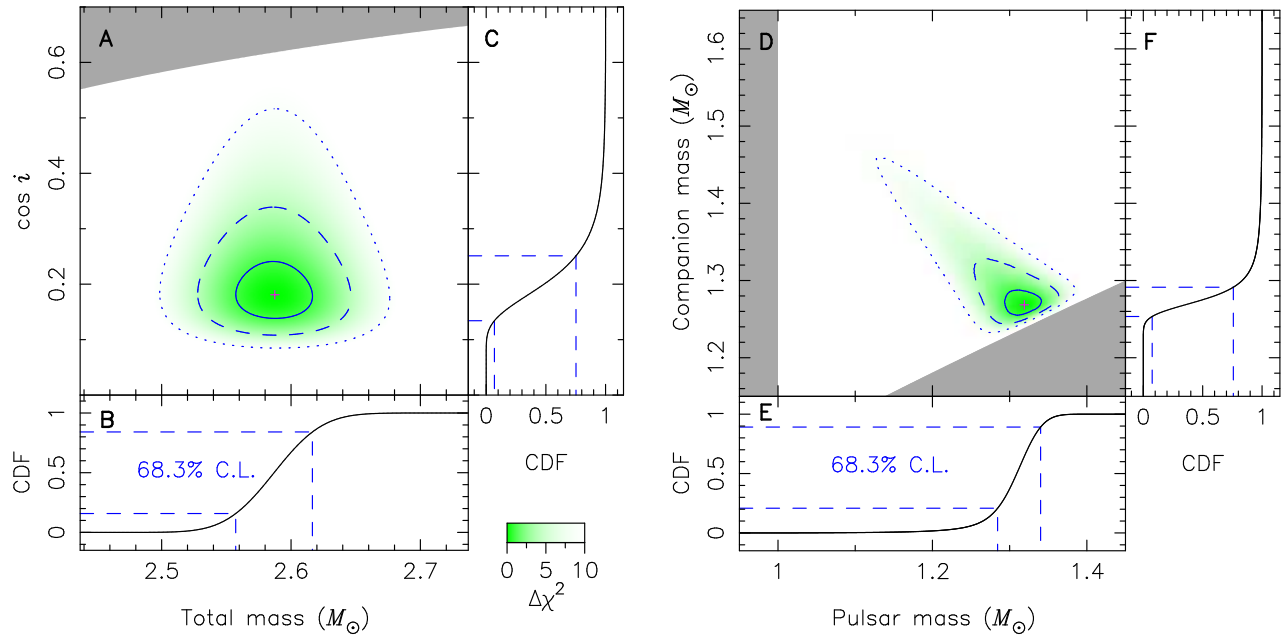


Figure 3. Constraints on the component masses and orbital inclination of PSR J0641+0448 derived from χ^2 analysis. The two-dimensional probability distributions in the $M_{\rm tot}$–cos i and $M_{\rm p}$–$M_{\rm c}$ planes are shown in subpanels (A) and (D), respectively. The contours correspond to $\Delta\chi^2$ levels of 1, 4, and 9. The best-fit values, $M_{\rm tot} = 2.588\ M_\odot$, $i = 79.^\circ6$, $M_{\rm p} = 1.319\ M_\odot$, and $M_{\rm c} = 1.269\ M_\odot$ are marked by red crosses. The highest density intervals containing 68.3% probability (enclosed by the blue dashed lines), derived from the one-dimensional cumulative distribution functions (indicated by the black lines) in panels (B), (C), (E), and (F), correspond to: $M_{\rm tot} = 2.557$ to 2.617 $M_\odot$, $i = 75.5$ to 82.3 deg, $M_{\rm p} = 1.284$ to 1.340 $M_\odot$, and $M_{\rm c} = 1.253$ to 1.291 $M_\odot$.

($M_{\rm tot}$, cos i), we calculated $M_{\rm c}$ using Equation (1) and then fitted the TOAs with the DDGR timing model (J. H. Taylor 1987; J. H. Taylor & J. M. Weisberg 1989) in which all other parameters were free to vary, and recorded the resulting $\Delta\chi^2 = \chi^2 - \chi^2_{\rm min}$. Here we have rescaled the χ^2 distribution so the minimum χ^2 is equal to the degree of freedom. The posterior probability density $p(M_{\rm tot}, \cos i)$ is then given by

$$p(M_{\rm tot}, \cos i) = \begin{cases} Ce^{-\Delta\chi^2/2} & M_{\rm p} > 1\ M_\odot \text{ if}, \\ 0 & \text{otherwise}, \end{cases} \quad (4)$$

where C is a normalization constant ensuring a total probability of unity. Using the mass function, we converted the $\Delta\chi^2$ distribution $\Delta\chi^2(M_{\rm tot}, \cos i)$ into $\Delta\chi^2(M_{\rm p}, M_{\rm c})$, which is shown in Figure 3(D). The gray region has been excluded as it corresponds to an unphysical $\sin i > 1$. The minimum χ^2 occurs at $M_{\rm tot} = 2.588\ M_\odot$, $i = 79.^\circ6$, $M_{\rm p} = 1.319\ M_\odot$, and $M_{\rm c} = 1.269\ M_\odot$, marked by the two red crosses in Figures 3(A) and (D). Integrating $p(M_{\rm tot}, \cos i)$, we obtained the following parameter ranges with a 68.3% confidence level (C.L.): $M_{\rm tot} = 2.557$ to 2.617 $M_\odot$, $i = 75.5$ to 82.3 deg, $M_{\rm p} = 1.284$ to 1.340 $M_\odot$, and $M_{\rm c} = 1.253$ to 1.291 $M_\odot$.

4. Discussion and Conclusion

We have reported the discovery, timing solution, and mass measurements of PSR J0641+0448, a mildly recycled pulsar with a spin period $P = 25.7$ ms, in a 3.73 day eccentric orbit ($e = 0.145$) around another neutron star, identified through the FAST GPPS survey. Based on 16 FAST observing sessions, we obtained a phase-connected timing solution and detected both periastron advance and Shapiro delay. Following E. M. Splaver et al. (2002), we performed χ^2 analysis based on the DDGR binary model, which constrained the pulsar mass to $1.319^{+0.021}_{-0.035}\ M_\odot$ and the companion mass to $1.269^{+0.022}_{-0.016}\ M_\odot$.

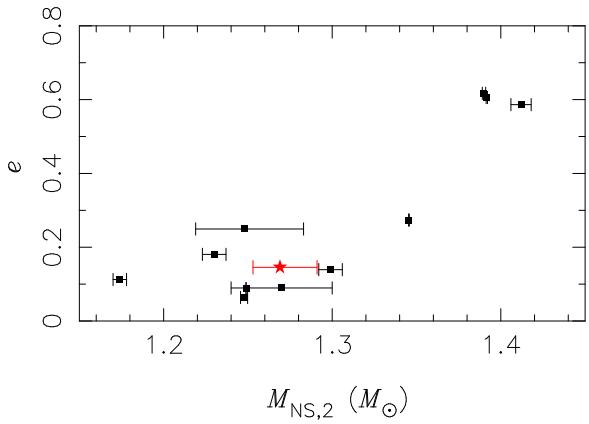


Figure 4. The masses of the second-born neutron star, $M_{\rm NS,2}$ and orbital eccentricities, e, of known DNS systems in the Galactic field. PSR J0641+0448 is marked by the red star. The error bars show the 1σ uncertainties of their masses.

In the future, continued follow-up observations of PSR J0641+0448 can improve the precision of the mass measurement. With a longer time span of about 10 yr, the Einstein delay parameters γ and the orbital period derivative $\dot{P}_{\rm orb}$ can be measured, which can be used to test general relativity and constrain the pulsar distance.

It has been proposed that core-collapse events involving stellar cores with low compactness, such as electron-capture supernovae, low-mass iron core-collapse supernovae, and ultrastripped supernovae with small metal cores, impart systematically smaller kicks than those from more massive iron-core progenitors (H.-T. Janka 2017; T. M. Tauris et al. 2017). Such smaller kicks are expected to yield lower orbital eccentricities, while the neutron

stars produced in these events are predicted to have lower masses (M. Ugliano et al. 2012; T. Sukhbold et al. 2016). This suggests a possible correlation between the mass of the second-born neutron star, $M_{\rm NS,2}$, and the orbital eccentricity e in DNS systems (T. M. Tauris et al. 2017).

To examine this correlation, we compiled $M_{\rm NS,2}$ and e values (see footnote[4]) from known Galactic DNS systems: PSRs J0453+1559 (J. G. Martinez et al. 2015), J0509+3801 (A. E. McEwen et al. 2024), J0737–3039A/B (M. Kramer et al. 2021), J1518+4904 (C. M. Tan et al. 2024), B1534+12 (E. Fonseca et al. 2014), J1756–2251 (R. D. Ferdman et al. 2014), J1757–1854 (A. D. Cameron et al. 2023), J1829+2456 (H. T. Haniewicz et al. 2021), J1913+1102 (R. D. Ferdman et al. 2020), B1913+16 (J. M. Weisberg & Y. Huang 2016), and J1946+2052 (L. Meng et al. 2025). As shown in Figure 4, a trend is visible between $M_{\rm NS,2}$ and orbital eccentricity. The position of PSR J0641+0448, which is marked by a red star, shows a low companion mass and moderate eccentricity, consistent with the proposed correlation.

Acknowledgments

This work made use of the data from FAST (https://cstr.cn/31116.02.FAST). FAST is a Chinese national mega-science facility, built and operated by the National Astronomical Observatories, Chinese Academy of Sciences. We all appreciate the excellent performance of the FAST and the operations team. The authors were supported by the National Key R&D Program of China No. 2025YFA1614000, National Natural Science Foundation of China (NSFC), grant Nos. 12588202 and 12041303, the Chinese Academy of Sciences via project JZHKYPT-2021-06, and the National SKA Program of China grant 2020SKA0120100 and 2022SKA0120103.

Facility: FAST.

Software: Presto (S. M. Ransom 2001), Dspsr (W. van Straten & M. Bailes 2011), Psrchive (A. W. Hotan et al. 2004).

ORCID iDs

Z. L. Yang https://orcid.org/0009-0009-6590-1540
J. L. Han https://orcid.org/0000-0002-9274-3092
P. F. Wang https://orcid.org/0000-0002-6437-0487
W. C. Jing https://orcid.org/0000-0002-1056-5895
W. Q. Su https://orcid.org/0009-0003-2212-4792
J. Xu https://orcid.org/0000-0003-1778-5580
Yi Yan https://orcid.org/0009-0008-1612-9948
D. J. Zhou https://orcid.org/0000-0002-6423-6106

References

Bhattacharyya, B., & Nityananda, R. 2008, MNRAS, 387, 273
Cameron, A. D., Bailes, M., Champion, D. J., et al. 2023, MNRAS, 523, 5064
Cordes, J. M., & Lazio, T. J. W. 2002, arXiv:astro-ph/0207156
Damour, T., & Deruelle, N. 1985, AIHPA, 43, 107
Damour, T., & Deruelle, N. 1986, AIHS, 44, 263
Damour, T., & Taylor, J. H. 1992, PhRvD, 45, 1840
Ferdman, R. D., Stairs, I. H., Kramer, M., et al. 2014, MNRAS, 443, 2183
Ferdman, R. D., Freire, P. C. C., Perera, B. B. P., et al. 2020, Natur, 583, 211
Fonseca, E., Stairs, I. H., & Thorsett, S. E. 2014, ApJ, 787, 82
Freire, P. C. C., & Ridolfi, A. 2018, MNRAS, 476, 4794
Han, J. L., Wang, C., et al. 2021, RAA, 21, 107
Han, J. L., Zhou, D. J., Wang, C., et al. 2025, RAA, 25, 014001
Haniewicz, H. T., Ferdman, R. D., Freire, P. C. C., et al. 2021, MNRAS, 500, 4620
Hobbs, G. B., Edwards, R. T., & Manchester, R. N. 2006, MNRAS, 369, 655
Hotan, A. W., van Straten, W., & Manchester, R. N. 2004, PASA, 21, 302
Hulse, R. A., & Taylor, J. H. 1975, ApJL, 195, L51
Janka, H.-T. 2017, ApJ, 837, 84
Kramer, M., Stairs, I. H., Manchester, R. N., et al. 2021, PhRvX, 11, 041050
Manchester, R. N., Hobbs, G. B., Teoh, A., & Hobbs, M. 2005, AJ, 129, 1993
Martinez, J. G., Stovall, K., Freire, P. C. C., et al. 2015, ApJ, 812, 143
McEwen, A. E., Swiggum, J. K., Kaplan, D. L., et al. 2024, ApJ, 962, 167
Meng, L., Freire, P. C. C., Stovall, K., et al. 2025, A&A, 704, A153
Nan, R. 2006, ScChG, 49, 129
Nan, R., Li, D., Jin, C., et al. 2011, IJMPD, 20, 989
Özel, F., & Freire, P. 2016, ARA&A, 54, 401
Özel, F., Psaltis, D., Narayan, R., & Santos Villarreal, A. 2012, ApJ, 757, 55
Park, R. S., Folkner, W. M., Williams, J. G., & Boggs, D. H. 2021, AJ, 161, 105
Pejcha, O., Thompson, T. A., & Kochanek, C. S. 2012, MNRAS, 424, 1570
Ransom, S. M. 2001, PhD thesis, Harvard Univ.
Sotomayor-Beltran, C., Sobey, C., Hessels, J. W. T., et al. 2013, A&A, 552, A58
Splaver, E. M., Nice, D. J., Arzoumanian, Z., et al. 2002, ApJ, 581, 509
Su, W. Q., Han, J. L., Yang, Z. L., et al. 2024, MNRAS, 530, 1506
Sukhbold, T., Ertl, T., Woosley, S. E., Brown, J. M., & Janka, H.-T. 2016, ApJ, 821, 38
Tan, C. M., Fonseca, E., Crowter, K., et al. 2024, ApJ, 966, 26
Tauris, T. M., & van den Heuvel, E. P. J. 2023, Physics of Binary Star Evolution: From Stars to X-ray Binaries and Gravitational Wave Sources (Princeton Univ. Press), http://www.jstor.org/stable/jj.8595663
Tauris, T. M., Kramer, M., Freire, P. C. C., et al. 2017, ApJ, 846, 170
Taylor, J. H. 1987, in Astronomical and Space Experiments to Test Relativity., in General Relativity and Gravitation, ed. M. A. H. MacCallum (Cambridge Univ. Press), 209
Taylor, J. H., & Weisberg, J. M. 1989, ApJ, 345, 434
Ugliano, M., Janka, H.-T., Marek, A., & Arcones, A. 2012, ApJ, 757, 69
van Straten, W., & Bailes, M. 2011, PASA, 28, 1
Wang, P. F., Han, J. L., Yang, Z. L., et al. 2025, RAA, 25, 014003
Weisberg, J. M., & Huang, Y. 2016, ApJ, 829, 55
Yao, J. M., Manchester, R. N., & Wang, N. 2017, ApJ, 835, 29
You, Z.-Q., Zhu, X., Liu, X., et al. 2025, NatAs, 9, 552